

# Simulation of Beam Instabilities in a Superconducting Linear Collider

Aune, A. Mosnier, O. Napoly  
DAPNIA/SEA  
CE Saclay France

## Abstract

We present some results on the short range and long range wakefields effects due to the SC cavities on a beam emerging from a TESLA linac [1]. In a first part, the intrabunch energy spread, which is affected by the rf curvature of the accelerating field and the longitudinal wake, is estimated after the usual linac phase optimisation. In a second part, multibunch transverse instability, which depends on the dipole cavity modes and their damping, is studied with several schemes of constant beta FODO focusing. In both cases, the parameters of a realistic 1.3 GHz TESLA cavity [2] and the parameters of the two machines "Top-Factory" and "1/2 TESLA" [3] are considered. We conclude that the longitudinal wake effect is not a problem in both machines and that a rather weak focusing scheme is sufficient to keep the emittance at the  $10^{-6}$  m rad design value.

## 1. THE MACHINE AND CAVITY PARAMETERS

We consider the two machines "Top-Factory" and "1/2 Tesla" defined in [3]. The useful parameters for energy spread and Beam Break Up calculations are listed in table 1.

Parameters	Top-Factory	1/2 Tesla
Energy / Linac (GeV)	125	250
Injection energy (GeV)	3	3
Bunch population	$2 \cdot 10^{10}$	$5.14 \cdot 10^{10}$
Bunch length (mm)	1	2
Number of bunches	800	800
Bunch separation ( $\mu$ S)	0.4	1.
Eacc (MV/m)	12.5	25
Tot number of cavities	10000	10000

Table 1 : List of the two machine parameters.

A 9-cell, 1.3 GHz cavity, with a 65 mm iris aperture, scaled from ref. [2] is considered. As the bunchlength is short, compared to the structure length, the short range longitudinal wakes are calculated with the code ABCI [4], which permits unequal mesh sizes in the axial and radial directions. The resulting total loss factors for one cavity are listed in table 2 and figure 1 shows the longitudinal wake for a  $\sigma=1$  mm gaussian bunch vs the longitudinal coordinate relative to the head of the bunch.

sigma (mm)	1	2
Kz tot (V/pC)	11.5	8.8

Table 2 : loss factors per cavity.

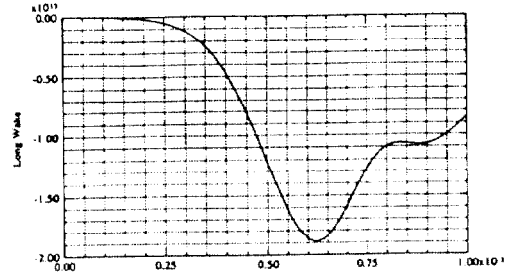


Figure 1 : Plot of the longitudinal wake in V/C ( $\sigma=1$ mm).

The dipole modes are calculated with the code URMEL [5] and, assuming a magnetic coupling, the anticipated loaded Q are estimated according the formulae :

$$Q_{ex} = \frac{\omega W}{P_{ex}} = \frac{2 R W}{\omega \mu^2 S^2 H_z}$$

where W is the mode stored energy, R is the load impedance, S is the loop area and  $H_z$  is the axial magnetic field at the coupler location. Table 3 gives the ten first highest coupling impedance non propagating dipole HOMs. Our definition for the transverse impedance ( in  $\Omega/m^2$  ) is :

$$R'/Q = \frac{1}{\omega W} \left| \int \nabla_{\perp} E_z e^{j k z} dz \right|^2 = \frac{2}{a^2} R'/Q_{Urmel}$$

where a is the distance from the beam axis at which the field is integrated.

Frequency (MHz)	R'/Q ( $10^4$ )	$Q_{ex}$ ( $10^4$ )
1890	11.7	5.0
1898	3.7	8.4
1881	7.1	3.2
1764	13.6	0.5
1906	0.2	34.2

Table 3 : R/Q and estimated  $Q_{ex}$  of the 5 first highest coupling modes.

Among the propagating modes, we have to worry about the trapped 5th passband, because these modes couple very poorly to the beam tube. If we assume the HOM couplers are located near the peak of the standing wave pattern of these modes, we find that only the very small R/Q modes are not at all damped.

## 2. ENERGY SPREAD CALCULATIONS

The total rms energy spread induced by the rf wavelength and by the longitudinal wake is minimized by proper choice of the linac phase. Figures 2 and 3 show the total rms energy spread for different longitudinal cuts of the bunch distribution, when the rf phase is varied.

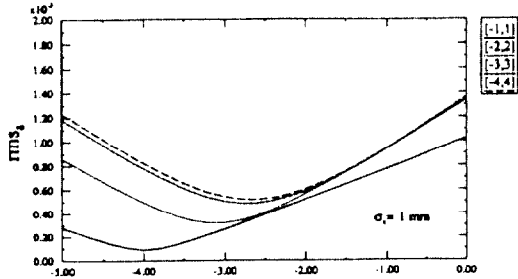


Figure 2 : total rms energy spread vs rf phase for the "Top-Factory" machine.

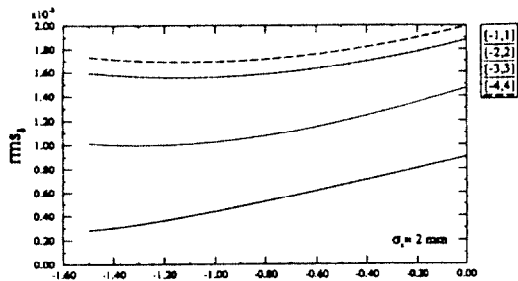


Figure 3 : total rms energy spread vs rf phase for the "1/2 TESLA" machine.

The rms energy spread due to the rf curvature only is estimated from the formula :

$$\frac{\sigma_E}{\langle E \rangle} = \frac{1}{\langle E \rangle} (\langle E^2 \rangle - \langle E \rangle^2)^{1/2} = (ch \sigma_\phi^2 - 1)^{1/2}$$

$$\frac{\sigma_E}{\langle E \rangle} \approx \frac{\sigma_\phi^2}{\sqrt{2}} \quad \text{with } \sigma_\phi = \frac{2\pi}{\lambda_{rf}} \sigma_z$$

The energy spreads due to the rf curvature only and due to the wake only and the final rms energy spread for particles between  $-4\sigma$  and  $+4\sigma$  after minimization by proper rf phase are listed in table 3. We note that the longitudinal wake effect was successfully compensated in the "Top Factory" machine, but not in the "1/2 Tesla" machine. In fact, the rf curvature effect is the dominant term and the wake is not strong enough for an effective compensation. Bunch too long or number of particles too low ? We checked that if the bunchlength is reduced to  $\sigma_z=1\text{mm}$ , the wake effect is higher and is able to compensate effectively the rf curvature effect (final rms energy spread =  $6.1 \cdot 10^{-4}$  for rf phase =  $-3.5^\circ$ ).

	Top-Factory	1/2 Tesla
rms energy spread induced by rf only ( rf phase = 0 )	$5.25 \cdot 10^{-4}$	$2.1 \cdot 10^{-3}$
rms energy spread induced by wake only	$1.4 \cdot 10^{-3}$	$1.2 \cdot 10^{-3}$
optimal rf phase	$-2.6^\circ$	$-1.2^\circ$
total rms energy spread after minimization	$5.15 \cdot 10^{-4}$	$1.7 \cdot 10^{-3}$

Table 3 : rms energy spreads for both machines.

## 3. THE MULTIBUNCH TRANSVERSE STABILITY

Following the idea in [6] , we study the multibunch instability generated by cavity misalignments rather than by offsets of the injected bunches. The train of 800 bunches is tracked through the 10000 cavities and the emittance growth is computed at the end of the linac. We have to check that the resulting emittance growth due to cumulative BBU is much smaller than the normalized horizontal emittance design value of  $10^{-6}$  m rad.

The coordinates of the bunch k at the entrance of the cavity N is given in terms of its coordinates at the entrance of the cavity N-1.

$$\begin{bmatrix} x_N(k) \\ x'_N(k) \end{bmatrix} = T_{N-1, N} \begin{bmatrix} x_{N-1}(k) \\ x'_{N-1}(k) \end{bmatrix} + \begin{bmatrix} 0 \\ \Delta p_\perp / p_{zN} \end{bmatrix}$$

where  $T_{N-1, N}$  is the transport matrix from the center of the cavity N-1 to the center of the cavity N and includes the adiabatic damping due to the acceleration. The kick given by the cavity N-1 is the result of the wakefields induced by all the preceding bunches :

$$\Delta p_\perp = \frac{e Q_b}{2} R'_\perp / Q \sum_{L=1}^{M-1} s_{M-L} x_{N-1}(L)$$

$$\text{with } s_K = e^{-k \omega_r \tau / 2Q} \sin k \omega_r \tau$$

The cavity alignment errors are randomly generated with a gaussian distribution. The standard deviation is fixed to  $\sigma_{\text{offset}} = 1 \text{ mm}$  with a distribution truncated at  $\pm 2\sigma$ . In the same way, as the mode frequency varies from cavity to cavity due to fabrication tolerances, each mode has a frequency dispersion of  $\sigma_{\text{freq}} = 1 \text{ MHz}$ . The frequency spread is far above the mode bandwidths ( about 50 times for a Q of  $10^5$  ) and is large enough to cancel any resonant buildup of the fields. We find that larger frequency spreads have no significant effect on the resulting emittance growth.

Simulations were performed for the two sets of parameters of table 1. The emittance dilution is larger (by a factor of 2 to 3) for the low energy case, as expected. Figure 6 shows for example the transverse displacements of the 800 bunches at the exit of the 10000-cavity linac with 10 HOMs and the phase space coordinates, from which the emittance growth is computed, is given on figure 7.

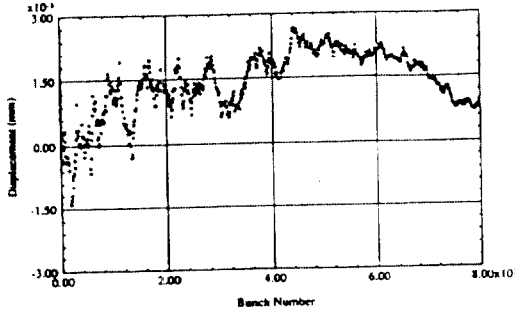


Figure 6 : Transverse displacement of the 800 bunches emerging from the linac

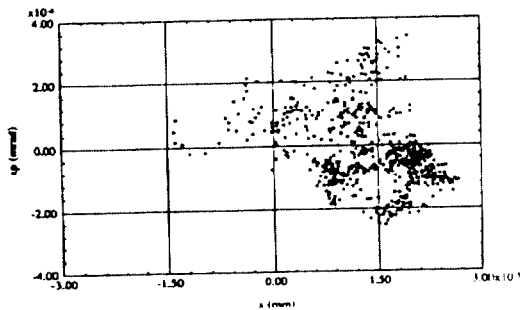


Figure 7 : Phase space coordinates of the 800 bunches emerging from the linac.

We studied the multibunch instability driven by the ten first highest coupling impedance non propagating modes. The focusing scheme is a constant cell length FODO lattice with constant phase advance and beta function all along the linac. In order to minimize the sensitivity to quadrupole misalignments, we looked for the lowest focusing strength which met the emittance growth requirement. We compute therefore the dependance of the emittance growth on the FODO lattice - length and phase advance - and on the Q of the modes.

### 3.1 The FODO cell length dependance

Since we find that the seed of the random generator, particularly for cavity position, has a significant effect on the blow up of the beam, the simulations are repeated several times with different seeds for each set of parameters. Figure 8 gives the normalized emittances for different seeds when the number of cavities between two adjacent quadrupoles is varied. The phase advance per cell was set to  $90^\circ$ . A module of 8 cavities is about 11 m long. The result is that the emittance growth vary approximatively linearly with the FODO cell length. We conclude that, with the Q's of table 3, a constant beta FODO lattice, with one quadrupole every 40th cavity

(55 m quadrupole spacing) is sufficient to guarantee an emittance dilution much smaller than the design value.

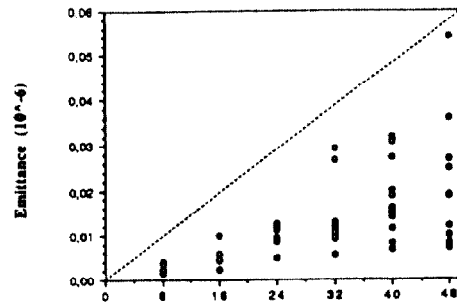


Figure 8 : Emittance growth vs the number of cavities per half FODO cell for  $\mu=90^\circ$ .

### 3.2 HOM external Q dependance

The number of cavities per half cell and the total number of quadrupoles are again set to respectively 40 and 250 and the same seed is used when the Qs are varied. The Qs of all the 10 modes are varied by the same factor. Figure 9 shows the increase of emittance with the Q. The Q value in abscissa is the Q of the first HOM of the table 3. We note a saturation of the blow up due to the finite pulse duration and that, as long as the Q of the first mode is lower than  $10^5$ , the emittance dilution is tolerable.

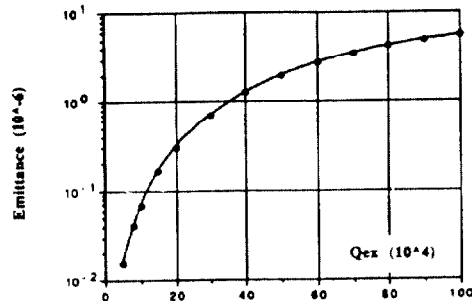


Figure 9 : Emittance growth with different  $Q_{ex}$ .

If we now include the effects of the six trapped modes plus the ten first non propagating modes, we obtain a maximum emittance growth of  $0.07 \cdot 10^{-6}$ , among the tested seeds, about 2 times higher than the emittance growth caused by only the 10 vanishing modes. We conclude that we have to pay special attention to the damping of the 5th passband modes in the design of the cavity.

## 4. REFERENCES

- [1] Proc. of the 1st TESLA Workshop, Cornell U., Ithaca, CLNS 90-1029, (1990)
- [2] E. Haebel and A. Mosnier, "Large or small iris aperture in SC multicell cavities ?" Proceedings of the 5th SRF Workshop, DESY, August 91
- [3] 2<sup>d</sup> TESLA Workshop, DESY Hamburg, August 1991
- [4] Y.H. Chin, CERN/LEP TH/88-3
- [5] T. Weiland, Nucl. Inst. and Meth. 216, 329 (1983)
- [6] G.A. Krafft et al., "Emittance growth in TESLA", Proceeding of the 1991 Part. Acc. Conf., San Francisco